Polymer Vol. 37 No. 7, pp. 1217–1228, 1996
Published by Elsevier Science Ltd
Printed in Great Britain
0032-3861/96/$15.00 + 0.00

Copolymer modification of nylon-6,6 with 2-methylpentamethylenediamine

Jan M. Stouffer, Howard W. Starkweather Jr, Benjamin S. Hsiao*, Peter Avakian and Glover A. Jones
DuPont Company, Central Research and Development, Experimental Station, Wilmington, DE 19880, USA
(Received 7 October 1994; revised 27 June 1995)

Polyamides were prepared in which part or all of the hexamethylenediamine (HMD) in nylon-6,6 was replaced by its isomer, 2-methylpentamethylenediamine (MPMD). The intermediate compositions are considered random copolymers between the two homopolymers (66 and MPMD-6). The crystalline properties of these polymers were studied by differential scanning calorimetry, X-ray diffraction and optical microscopy. It was concluded that the two kinds of units, 66 and MPMD-6, do not co-crystallize. In copolymers containing large fractions of HMD, the MPMD units are excluded from the crystals. With appropriate thermal treatment, MPMD-6 can crystallize with two different unit cells and a variety of spherulitic morphologies. The two crystal forms can be distinguished by their crystallization, melting and optical properties. The crystallization kinetics of the copolymers are slower than those of the homopolymers, which is associated with the slower rate of nucleation formation rather than the transport ability. This is consistent with the dielectric results, which showed that the glass transition temperatures of the different copolymers are similar. It was found that MPMD-6 can be quenched into an amorphous state. The properties of the amorphous portions were further investigated through dielectric relaxations. Although, the incorporation of MPMD tends to shift the dielectric gamma relaxation towards higher temperatures, the total effects of variations on chemical structure were much smaller than those which pertain to the crystalline phase.

(Keywords: nylon-6,6 copolymers; 2-methylpentamethylenediamine; characterization; crystal structure; morphology)

INTRODUCTION

2-Methylpentamethylenediamine (MPMD) is an isomer of hexamethylenediamine (HMD). It is sold by DuPont under the tradename Dytek® A and can be used as a polymer intermediate in the same manner as other aliphatic diamines. We have examined the thermal properties of a series of copolymers in which MPMD was substituted for part of the HMD in nylon-6,6 as well as MPMD-6, the homopolyamide made from MPMD and adipic acid.

Much of the interest is centred on the way in which the incorporation of units of MPMD affects the crystalline structure of nylon-6,6 and how the homopolymer can crystallize. These issues were addressed principally by X-ray diffraction, differential scanning calorimetry (d.s.c.) and optical microscopy. The effect of structure on the properties of the amorphous regions in this family of polyamides was assessed through dielectric analysis. Morphological features were characterized mainly through the observation of spherulitic appearance. The effect on the crystallization kinetics was studied by two separate approaches: the bulk cyrstallization rate using thermal analysis, and the spherulite growth rate using optical microscopy.

* To whom correspondence should be addressed

EXPERIMENTAL

Materials and preparation

The chosen samples were developmental-grade nylon-6,6 copolymers with 2-methylpentamethylenediamine (MPMD). Nine compositions of HMD/MPMD were prepared: 100/0, 90/10, 80/20, 65/35, 60/40, 40/60, 30/70, 20/80 and 0/100. The 100/0 ratio is the homopolyamide of nylon-6,6, and the 0/100 ratio is the homopolyamide of the nylon MPMD-6. The intermediate compositions are considered random copolymers between the two homopolymers. Their mean weight-average molecular weight is 24 000 with polydispersity of about 2.

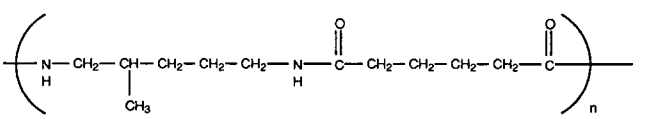

MPMD-6

All samples were vacuum dried at 80°C for 24 h prior to any preparation or measurement. The films (thickness about 5 μm) were prepared by melt pressing powder specimens at approximately 20°C above the apparent melting temperature for optical microscopic measurements. For the Hoffman–Weeks analysis, samples were analysed after completion of the isothermal crystallization kinetics measurements. Thicker films (about

1 mm) were melt crystallized for X-ray measurements. Polymer samples for the dielectric experiments were dried overnight under nitrogen at 100°C, then films 200–400 μm thick were made by pressing the polymers between sheets of Kapton® on a hot plate at 270°C.

Characterization techniques

Two different thermal analysis stations were used: a TA 990 DSC to measure the routine heating scans, and a Perkin-Elmer DSC7 to study the crystallization rate. In the latter measurement, samples were first equilibrated at about 20°C above their nominal melting temperatures for 10 min and were subsequently cooled at a rate of 320°C min^{-1} to the desired temperature. The isothermal crystallization peak time was recorded to characterize the crystallization rate. The peak time was determined at the time when the exothermic heat flow reached a maximum in the isothermal scan. For the typical d.s.c. run, the heating rate of 10°C min^{-1} was used unless otherwise specified. All thermal scans were conducted under a nitrogen environment.

The spherulite growth rate was measured by a polarizing optical microscope (Nikon Optiphot-PDL) equipped with a video camera and a Mettler FP82 HT hot stage (up to 400°C). The experimental conditions used were similar to the d.s.c. crystallization peak time measurements. Video images of the crystal growth were digitized by JAVA video analysis software (Jandel Scientific, CA) with a PC station. A first-order red tint plate was adopted to determine the sign of spherulite birefringence under cross-polarization.

Room-temperature X-ray diffractometry scans were collected in the symmetrical transmission mode using an automated Philips diffractometer (curved crystal monochromator, 1° divergence and receiving slits, sample rotating) and Cu Kα radiation. Data were collected in a fixed time mode with a step size of 0.05° and run from $2\theta = 4°$ to 65°. Reflection positions were defined by deconvoluting the diffraction pattern into a series of Gaussian peaks. The diffraction pattern from the non-crystalline phase was extracted and subtracted from the semicrystalline pattern. The X-ray data at elevated temperatures were obtained with a Rigaku theta–theta diffractometer in which the sample remains in the horizontal plane, with the X-ray source and the detector moving through corresponding angles in a vertical plane[1].

For the dielectric measurements, the films were clamped between phosphor bronze disc electrodes (16 mm diameter) in a custom-built variable-temperature dielectric cell using liquid nitrogen cooling and electrical heating in conjunction with a Lake Shore Cryotronics model DRC 82C temperature controller. Before each measurement, the sample was dried by heating the nitrogen-filled dielectric cell to 160°C, then kept at that temperature for about 15 min. The dielectric measurements were performed with a C. Andeen Associates Impedance Measuring Bridge (model CGA-85) with 17 frequencies covering the range 10 Hz to 100 kHz plus a PC. During the dielectric scans, the temperature of the sample was ramped upwards at 0.5°C min^{-1}.

RESULTS AND DISCUSSION

Properties of the crystalline phase in copolymers

In *Figure 1*, X-ray diffractometer scans are compared

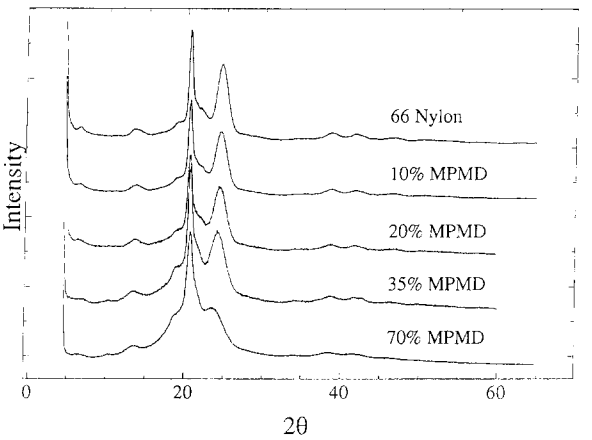

Figure 1 X-ray diffractometer scans on 66/MPMD-6 nylon copolymers

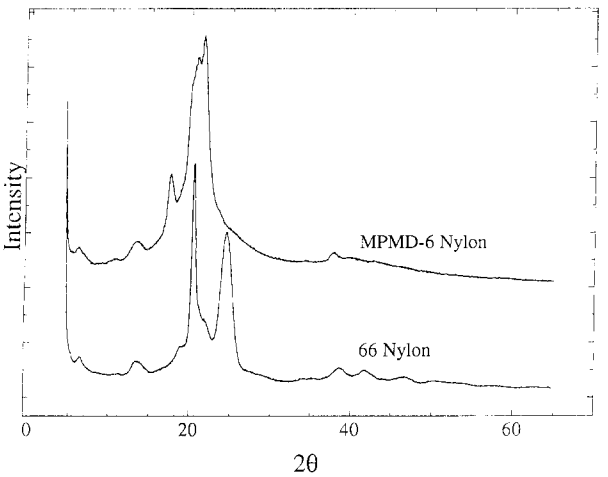

Figure 2 Comparative X-ray diffractometer scans for 66 and MPMD-6 homopolymers

for a homopolymer of nylon-6,6 (also denoted 66) and copolymers containing from 10 to 70% MPMD in the diamine moiety. Since HMD and MPMD are isomers, the weight and mole fractions are the same. The locations of the principal peaks are nearly unchanged. Note the following strong reflections: (0 0 2) at 13.5°, (1 0 0) at 20.5°, (0 1 7) at 38.7° and (1 1 7), (0 2 7) at 42°, using the triclinic unit cell where $a = 4.9$ Å, $b = 5.4$ Å, $c = 17.2$ Å, $\alpha = 48.5°$, $\beta = 77°$ and $\gamma = 63.5°$ (ref. 2). The (0 1 0), (1 1 0) doublet at 24° moves to a slightly lower angle in the copolymer with 70% MPMD, its intensity also decreases significantly. This figure indicates that the 66 crystals persist in the copolymers even with high MPMD content. It is apparent that the copolymer of 70% MPMD consists of a mixture of 66 and MPMD-6 crystals, the properties of which will be discussed later.

Major changes are seen for the homopolymer of MPMD-6 in *Figure 2*. There are peaks close to the (0 0 2) and (1 0 0) reflections in nylon-6,6, but well defined new peaks appear at 17.5°, 21.45° and 38°. It is clear that, while MPMD-6 is well able to crystallize, the crystal structure of nylon-6,6 is dominant in the copolymers. In *Figure 1*, we do not find any experimentally significant variations in the peak positions for the

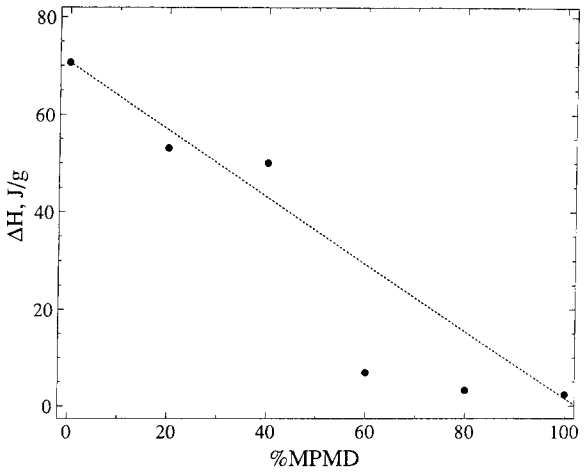

Figure 3 The effect of MPMD on the net heat of fusion in copolymers of nylon-6,6; specimens quenched rapidly from the melt

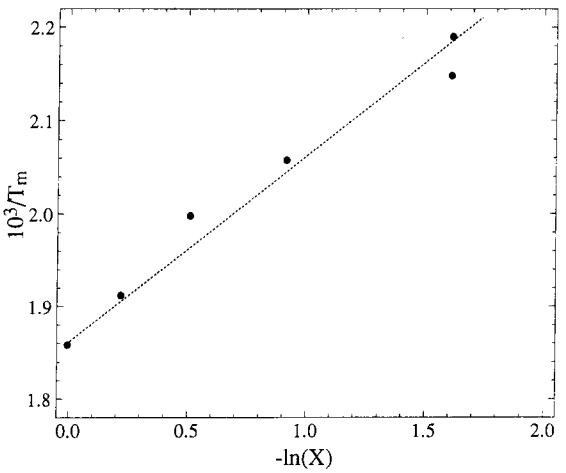

Figure 4 The effect of composition on the melting point of 66/MPMD-6 nylon copolymers; X = mole fraction of nylon-6,6 units

various copolymers prepared under a similar condition. This indicates that co-crystallization between the units of 66 and MPMD-6 probably does not occur. This is consistent with the results in *Figure 2*, which show that crystallographic repeat lengths in 66 and MPMD-6 are significantly different, making co-crystallization unlikely.

When d.s.c. scans are run on samples that have been cooled rapidly from the melt, there may be one or more crystallization exotherms followed by one or more melting endotherms. The net heat of fusion (endotherms minus exotherms) is indicative of the level of crystallinity at room temperature. This quantity is plotted against percentage of MPMD in *Figure 3*. Up to 40% MPMD the net heat of fusion is approximately proportional to the fraction of nylon-6,6 in the copolymers. At 60–100% MPMD, the net heat of fusion and thus the percentage crystallinity in samples cooled rapidly from the melt is very low.

The depression of the melting point in copolymers from the above measurement can be described by the following equation due to Flory[3,4]:

$$\frac{1}{T_m} - \frac{1}{T_m^\circ} = -\left(\frac{R}{\Delta H_u}\right) \ln X \qquad (1)$$

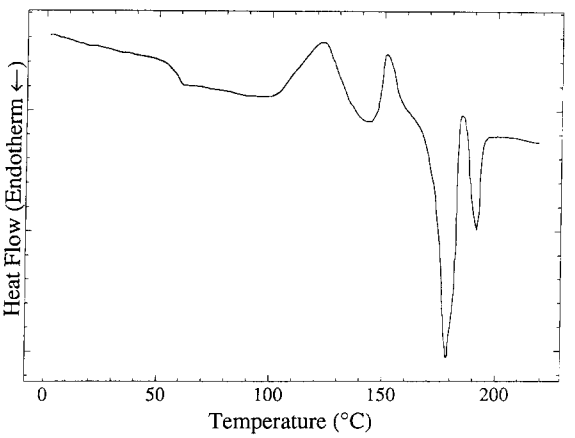

Figure 5 D.s.c. scan for MPMD-6 after rapid cooling from the melt

T_m and T_m° are the melting points in kelvin of the copolymer and homopolymer, respectively; ΔH_u is the heat of fusion per repeat unit of the major component; and X is the mole fraction of the major component (all the variables are in thermodynamic equilibrium). This equation is valid only if the comonomer units are excluded from the crystals. The data for the 66/MPMD-6 copolymers are plotted in this form in *Figure 4*. For this purpose, T_m is taken as the end of the melting interval where the last crystal is presumed to be in equilibrium with the melt. Our intention here is only to examine whether the copolymer crystals include or exclude the MPMD units. A further examination of the equilibrium melting temperature for different compositions will be discussed later using the Hoffman–Weeks approach. In *Figure 4*, the data points corresponding to 0–80% MPMD-6 lie close to a line corresponding to a heat of fusion of 45 cal g^{-1} (188 J g^{-1}). This is the value for the heat of fusion for the crystalline phase of nylon-6,6 as determined by application of the Clapeyron equation[5]. In this case, we conclude that MPMD units are most probably excluded from the crystals in the compositions of 0–80% MPMD-6.

The X-ray patterns, net heats of fusion and the melting points are all consistent with the hypothesis that the units of MPMD-6 are excluded from the crystals of nylon-6,6. This is reasonable, because the units of MPMD-6 are shorter than those of nylon-6,6. The chains in the crystals of nylon-6,6 are fully extended[2]. There is no way that a shorter unit can be included in that crystal without a major rearrangement of adjacent chains. The effect of the methyl side groups is probably less serious, since they can be accommodated in crystals of other polymers through adjustments of lattice parameters[6–11].

Properties of the crystalline phase in MPMD-6 homopolymer

Figure 5 is a d.s.c. scan for a sample of MPMD-6 that had been cooled rapidly from the melt to below room temperature. There are two exotherms at about 120 and 150°C followed by two endotherms at 178 and 190°C. There appears to be an additional small exotherm between the endotherms at 184°C. These data suggest that there are two separate crystalline forms each having characteristic crystallization and melting temperatures. Some of the lower-melting form appears to recrystallize after melting to add to the higher-melting form. The net

Table 1 Peak positions[a] in high-temperature powder patterns

D.s.c. response	Temperature (°C)	Peak 1	2	3	4	5	6
	25				19.7		
	80				19.85	20.6	
1st exo	100		17.05				20.95
1st exo	125	12.75	17.05				20.95
1st exo	143	13.6	17.0		19.65		20.85
2nd exo	152	13.05	17.0		19.7		20.95
2nd exo	160	13.05	16.9		19.5	20.5	21
2nd exo	165	13.5	16.7	18.5	19.65	20.45	20.95
1st endo	170	13.5	16.85	18.45	19.6	20.5	21.0
1st endo	175		16.8	18.3	19.55		20.95
1st endo	180		16.85	18.4	19.55	20.3	20.95
1st endo	184		16.7	18.35	19.55	20.4	20.95
2nd endo	187				19.15		
2nd endo	192				19.15		

[a] Most peaks may be assumed due to equatorial reflections. Form I: Peaks 1,2,4,6. Form II: Peaks 3,5,6

heat of fusion, that is, the latent heats of the endotherms minus those of the exotherms, is close to zero, showing that the original state at room temperature was highly, if not completely, amorphous. It is also observed that the enthalpy change of the 120°C exotherm is similar to that of the 178°C endotherm, and the change of the 150°C exotherm is close to that of the 190°C endotherm. This indicates that the former relationship probably represents the transition of the lower-temperature crystal form I, and the latter is the transition of the higher-temperature form II.

X-ray diffractometer scans were obtained over a temperature range from 25 to 192°C. The peak positions observed at each temperature are listed in *Table 1*. Peaks at 13°, 17.0° and 19.65° in 2θ were associated with the first exotherm and the first endotherm (form I), and peaks at 18.4° and 20.5° were associated with the second exotherm and the second endotherm (form II). Both forms had a peak at 20.95°. In *Table 1*, it is seen that the first peak (2θ ca. 13°) increases with temperature, whereas the remaining peaks decrease (except the last peak at 20.95°, which is about constant). Since in nylon-6,6, the temperature effect is known to increase the a and b axes (thus decreases the 2θ values) and decrease the c axis, it is logical to assume that the first peak (13°) is related to the 001 reflection and the remaining peaks are related to the $hk0$ reflections.

The reflections at 17–21° were interpreted as the 0 1 0, 1 1 0 and 1 0 0 reflections from putative monoclinic unit cells. Logically, a triclinic cell may be present; herein we used the simpler monoclinic cell to estimate the crystal densities of the two polymorphs. Thus,

$$d_{hk0}^{-2} = \frac{(h/a)^2 + (k/b)^2 - (2hk/ab)\cos\gamma}{\sin^2\gamma} \quad (2)$$

$$d_{100} = a\sin\gamma \text{ and } d_{010} = b\sin\gamma \quad (3)$$

$$d_{110}^{-2} = \frac{a^{-2} + b^{-2} - (2/ab)\cos\gamma}{\sin^2\gamma} = d_{100}^{-2} + d_{010}^{-2} - \frac{2\cos\gamma}{d_{100}d_{010}} \quad (4)$$

The results of treating these data in terms of equations (3)–(5) are given in *Table 2*. The a parameter, the interchain separation within the hydrogen-bonded sheets, is about 4.8 Å in both forms. This is about the same as $a\sin\beta$, the corresponding quantity for the triclinic unit cell in nylon-6,6. In nylon-6,6, $b\sin\alpha$, the separation between chains in adjacent sheets, is significantly smaller, slightly more than 4 Å. This is because the hydrogen bonds hold the chains further apart than they would otherwise be. In MPMD-6, the b parameter is much larger, 5.94 Å and 5.44 Å for the lower- and higher-melting forms, respectively.

There is a second-order meridional reflection in fibre patterns at $2\theta = 13.2 \pm 0.3°$ that is similar to the 0 0 2 reflection in nylon-6,6. Thus, the c parameter in a monoclinic unit cell would be 13.4 ± 0.3 Å. Since the volume of a monoclinic unit cell is $abc\sin\gamma$, the density, assuming that the cell contains one chemical repeat unit, would be 1.11 ± 0.03 g cm^{-3} for the lower-melting form I and 1.21 ± 0.03 g cm^{-3} for the higher-melting form II. The literature values for the crystalline density of nylon-6,6 are 1.24 ± 0.04 g cm^{-3} from ref. 2, 1.213 ± 0.006 g cm^{-3} from ref. 12 and 1.220 ± 0.002 g cm^{-3} from ref. 13.

Thus, the higher-melting crystalline form II in MPMD-6 appears to be almost as dense as the crystal of nylon-6,6. The form I, which crystallizes and melts at lower temperatures, has a significantly lower density, as might have been expected.

MPMD-6 is an odd–even polyamide. To form all of the hydrogen bonds in a manner analogous to the even–even polyamides, there must be a 180° twist within the diamine moiety. This will tend to shorten the chemical repeat length in the crystal. MPMD contains an asymmetric carbon atom, and the diamine used here

Table 2 Equatorial monoclinic parameters for MPMD-6

	hkl (0 1 0)	(1 1 0)	(1 0 0)	a (Å)	b (Å)	γ (deg)
First crystalline form I						
2θ (deg)	17.00	19.65	20.95			
d (Å)	5.22	4.52	4.24	4.83	5.94	61.33
Second crystalline form II						
2θ (deg)	18.40	20.50	20.95			
d (Å)	4.82	4.33	4.24	4.79	5.44	62.42

	Reference	$a\sin\beta$ (Å)	$b\sin\alpha$ (Å)
Literature values for nylon-6,6	2	4.77	4.04
	12	4.84	4.09

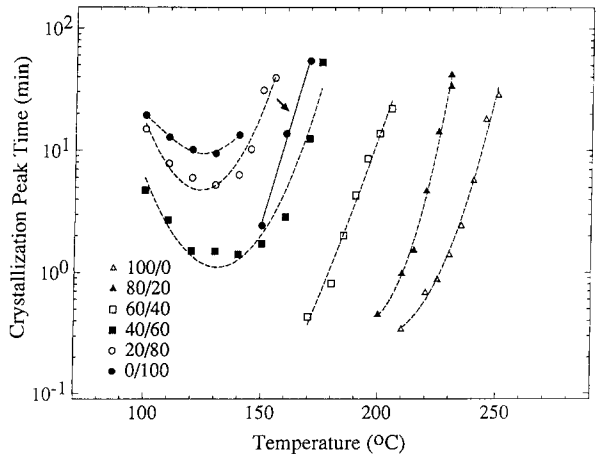

Figure 6 Isothermal crystallization peak time analysis for different 66/MPMD-6 compositions using d.s.c. technique

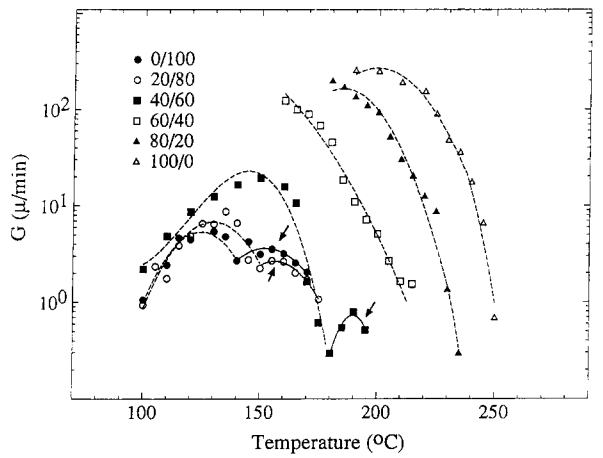

Figure 7 Isothermal spherulite growth rate analysis for different 66/MPMD-6 compositions using optical microscopy. The dotted lines represent the spherulites with Maltese cross patterns, the solid lines represent the spherulite aggregates

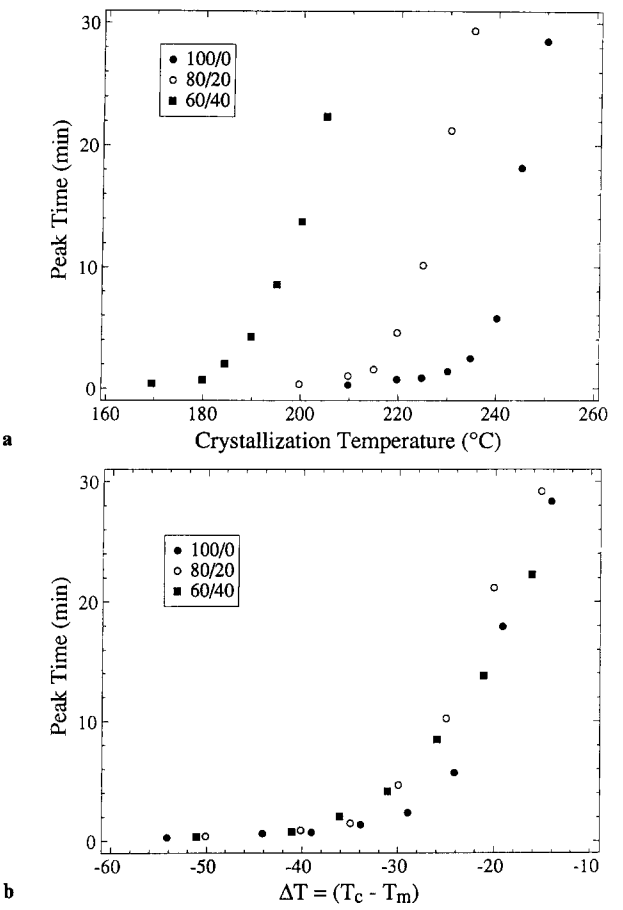

Figure 8 Effect of crystallization temperature on crystallization rate for 66/MPMD copolymers. (a) Crystallization peak time *versus* crystallization temperature. (b) Crystallization peak time *versus* undercooling ($T_c - T_m$)

is believed to be a mixture of the two steric isomers. Moreover, it is believed that the two ends of the diamine enter the polymer chain at random. Thus, the methyl side groups are thought to be distributed among four possible positions. In view of these factors, it is not surprising that MPMD-6 is easily quenched to an amorphous state and, when it is crystallized, that the reflections in a fibre pattern are limited to the equator and the meridian.

Crystallization kinetics

The bulk crystallization peak time (reciprocally proportional to the crystallization rate) *versus* temperature plot for different 66/MPMD-6 compositions is shown in *Figure 6*. Several features are identified here. The compositions from 100/0 to 60/40 (HMD/MPMD) do not show a maximum crystallization rate temperature. This may be because their maximum rates are simply too fast to be detected by d.s.c. In contrast, the compositions from 40/60 to 0/100 exhibit the maximum rate temperatures at a similar value about 130°C. The observation of the maximum crystallization behaviour is attributed to the decrease in the crystallization rate by increasing the MPMD content. It is conceivable that the MPMD-6 moieties not only introduce conformational hindrance during crystallization, but also decrease the possibility of forming available nucleating sites. An interesting phenomenon is observed in MPMD-6, i.e. at crystallization temperatures above 140°C, faster crystallization rates again occur (see arrow in *Figure 6*). As a result, a double-peak crystallization rate feature was observed, which can be attributed to the crystallization of two different polymorphs in MPMD-6.

The corresponding spherulite growth rate *versus* temperature plot (determined by thermal optical analysis) for different compositions is shown in *Figure 7*. The features in *Figure 7* are generally similar to those in *Figure 6*. The isothermal growth rate is significantly retarded by the introduction of the MPMD moieties. Only the compositions from 40/60 to 0/100 show a maximum growth rate behaviour, while those from 100/0 to 60/40 do not. The growth rate data of nylon-6,6 are consistent with the earlier published results[14]. In *Figure 7*, we also find two maximum growth rates present in the compositions from 40/60 to 0/100. The lower-temperature growth rate region is indicated by the dotted line and the higher-temperature region is indicated by the solid line and the arrow symbol. These two regions represent two different types of spherulites: optically regular spherulites with Maltese-cross patterns at lower

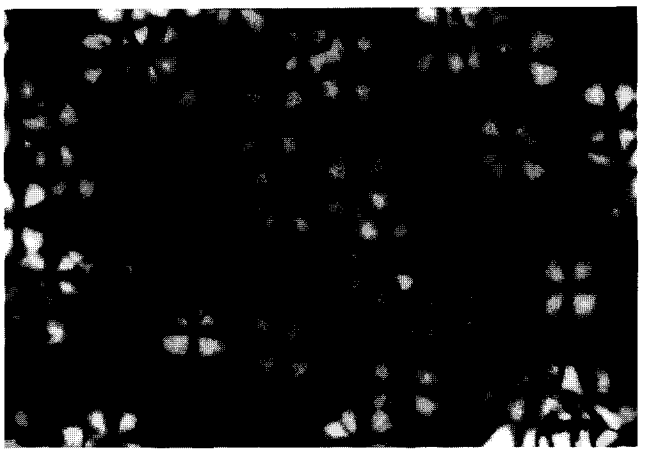

Figure 9 Positive non-ringed spherulites grown at 185°C in the 60/40 composition after fusion at 280°C for 5 min

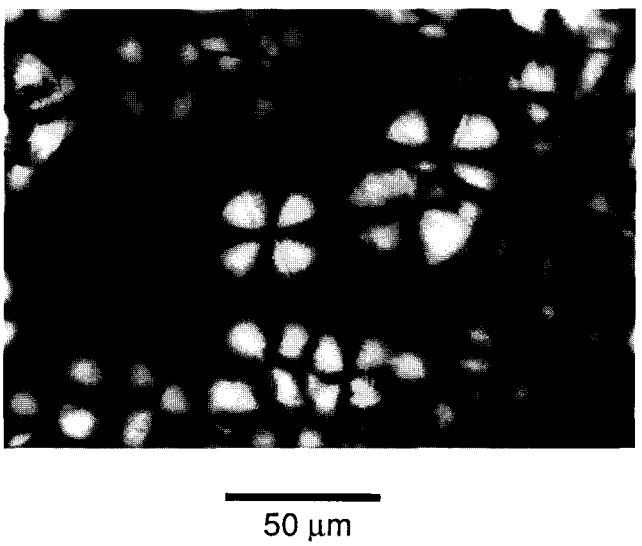

Figure 10 Positive ringed spherulites grown at 185°C in the 80/20 composition after fusion at 280°C for 5 min

temperatures, and spherulite aggregates with no preferred optical orientation at higher temperatures. The faster-growing spherulite aggregates have been observed before in 66 and other nylons[15–18].

From the crystal growth theory[19], the growth rate can be divided into two separate processes, the transport of the crystallizing species across the amorphous–crystal boundary and the formation of the crystal entity. Since the glass transition temperatures of the different copolymers are found to be about the same, the transport process must be virtually unchanged by MPMD. The effect of crystallization temperature on the crystallization rate of the copolymers is shown in *Figure 8*. In the plot of crystallization peak time *versus* crystallization temperature for different copolymers (*Figure 8a*), it appears that increasing the content of MPMD increases the time to crystallize at a given temperature (data extracted from *Figure 6*). This is not the best comparison, because we know that MPMD lowers the melting point and therefore decreases the undercooling at a given crystallization temperature. We see in *Figure 8b*, a plot of peak time *versus* undercooling ($T_c - T_m$), that the crystallization rate is the same for copolymers with up to 40% MPMD, if we normalize to the undercooling. Thus, the growth-rate-dominating process must be the nucleation. We conclude that the retardation of the nucleation due to MPMD is associated with the increase in the free energies of crystal formation. This may be due to the decrease in the effective degree of undercooling or the increase in the crystal surface free energies. In either case, it is necessary to investigate the equilibrium melting temperature for each composition, which will be discussed later. From the optical microscopy measurements, the density of spherulitic nuclei was clearly decreased with the increase in MPMD content. This was consistent with the argument that increasing the content of MPMD decreases the ability to form crystals.

Figure 11 Ringed spherulites with a zigzag extinction grown at 155°C in the 20/80 composition after fusion at 240°C for 5 min

Spherulite morphology

Similar to the reported spherulite morphologies in the nylon-6,6[15,18,20], there are at least four types of spherulites in 66/MPMD-6 copolymers depending on the crystallization temperature as well as the composition. These morphologies are summarized as follows.

The typical spherulite appearance in the copolymers shows a positive birefringence with either ringed or non-ringed texture under cross-polars. In the composition of high 66 content ($\geq 60\%$), the non-ringed spherulites, which have straight extinction cross patterns, are usually observed as shown in *Figure 9*. This morphology is attributed to the preferred alignment of the crystallographic *a* axis (hydrogen-bonding direction) along the spherulite radii[17,21,22], leading to a larger radial refractive index and thus a positive birefringence. The ringed spherulites are also observed in these compositions, but only at lower crystallization temperatures and limited to a narrow temperature range. *Figure 10* shows typical ringed spherulite morphology in the composition of 80/20. The average ring spacing increases and the ring texture coarsens with increasing crystallization temperature,

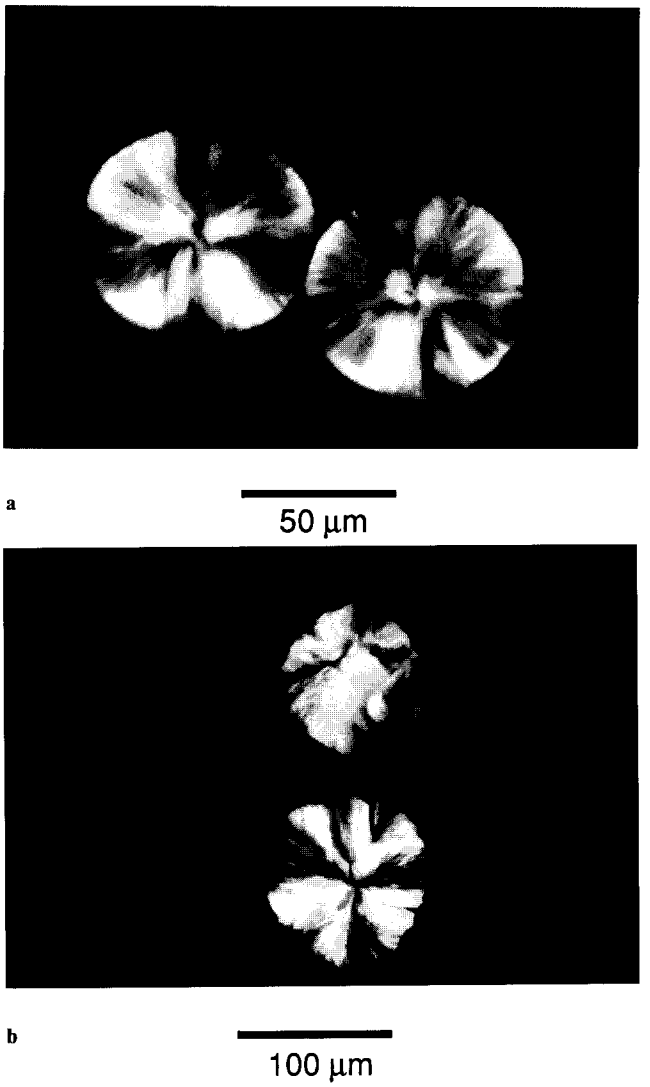

Figure 12 (a) Positive spherulites grown at 185°C and (b) negative spherulites grown at 195°C, in the 40/60 composition after fusion at 260°C for 5 min

which has been reported in nylon-6,6 before[17]. The ringed textures have been attributed to a cooperative twisting of crystalline ribbons along the growth axis. In addition, we have observed both ringed and non-ringed spherulites coexistent at some crystallization temperatures.

In the low 66 compositions ($\leq$ 40%), a different type of the ringed spherulite (also with a positive birefringence) is observed. At lower crystallization temperatures, the typical Maltese cross patterns are seen but with a slight distortion, which exhibit a similar ringed morphology as previously observed in the high 66 compositions. As the temperature is increased, these patterns show a zigzag extinction as seen in *Figure 11*. In fact, a spiral morphology can be identified, which is identical to the one found in nylon-5,6[16]. The growth rate of the spherulite with a distinct zigzag extinction can be faster than that without it, even though the former is at a higher crystallization temperature (*Figure 7*). The strength of the birefringence in the spiral spherulite is usually higher than its lower-temperature counterpart. The spacing of the spiral also increases with crystallization temperature. At high crystallization temperatures near the melting

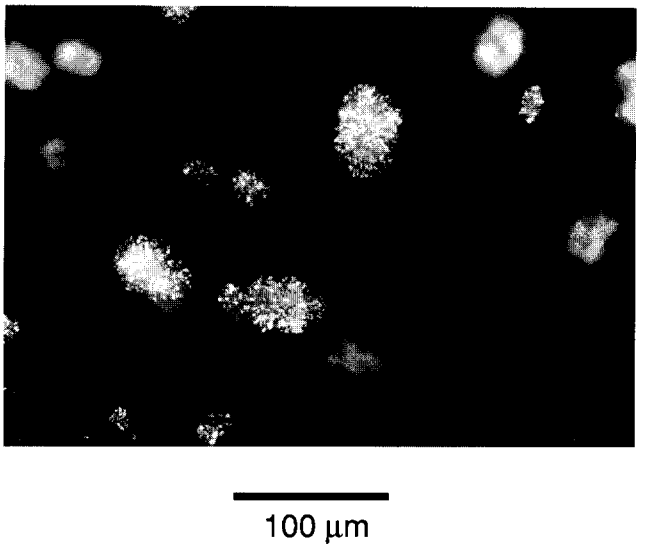

Figure 13 Spherulite aggregates grown at 160°C in the 20/80 composition after fusion at 240°C for 5 min

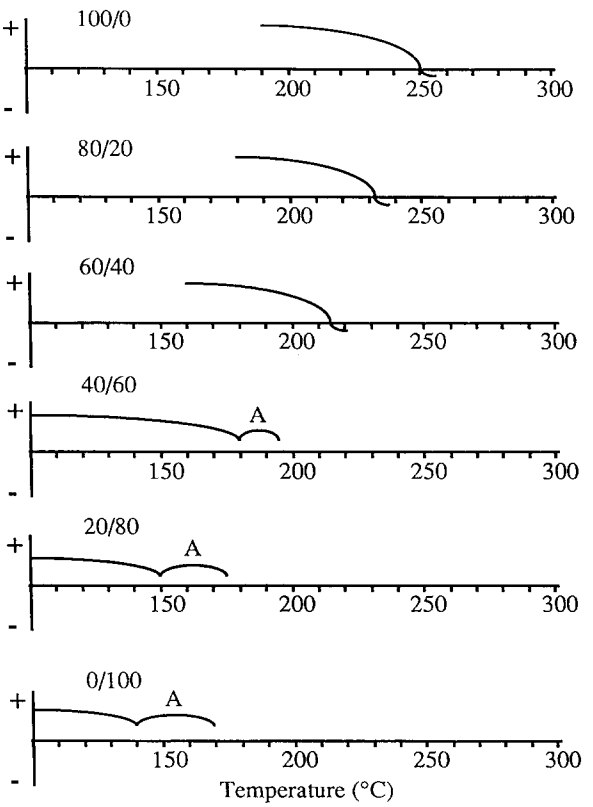

Figure 14 Schematic summary of spherulite birefringence as a function of temperature in different compositions. The symbol A represents the spherulites with distinct zigzag extinction (spiral textures)

point the spiral morphology eventually becomes diffuse with low birefringence.

We have observed negative birefringent spherulites grown at high crystallization temperatures in compositions from 100/0 to 40/60 (HMD/MPMD). *Figure 12* shows the typical positive spherulites at 185°C (a) and the negative spherulites at 195°C (b) in 40/60. We found that the negative spherulites were present only at

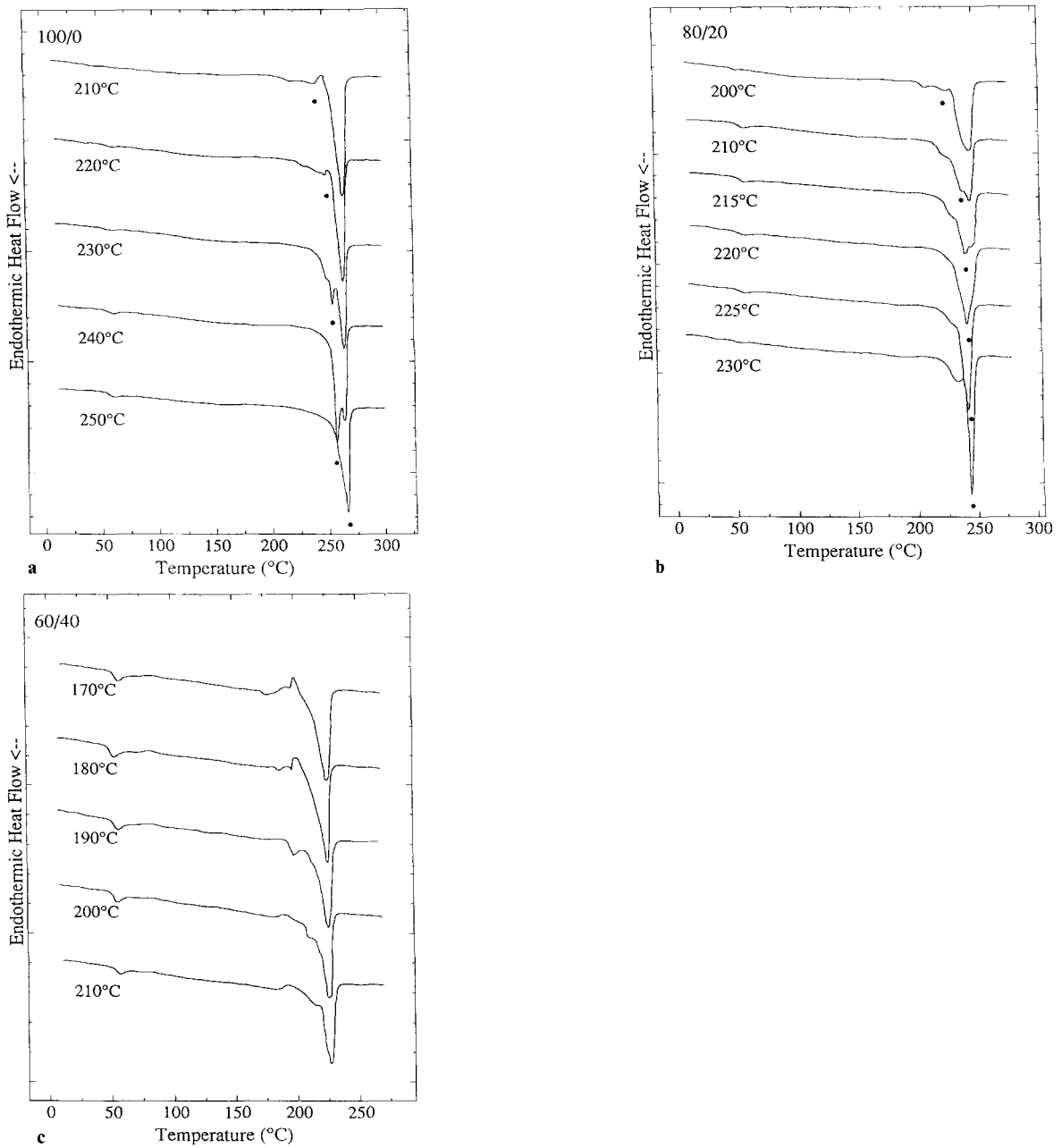

Figure 15 D.s.c. scans of isothermally crystallized samples at different temperatures for the compositions of (a) 100/0, (b) 80/20 and (c) 60/40. The symbol (●) represents the increasing trend of nominal melting point by T_c

higher crystallization temperatures: 100/0, $\geq 250°C$; 80/20, $\geq 235°C$; 60/40, $\geq 220°C$; 40/60, $\geq 195°C$. No negative spherulite could be identified in the compositions of 20/80 and 0/100. The negative spherulites were found to be coexistent with the positive spherulites. The former usually have a slightly faster growth rate and a higher optical melting temperature for the same crystallization temperature. It has been shown that, in nylon-6,6, the negative spherulites are due to the loss of preferred *a*-axis alignment in the spherulite radial direction[21]. In other words, although these spherulites may be more crystalline, there is little preferred orientation of the unit cells leading to a reduction in refractive index along the radii. Between the positive and the negative spherulites, there must lie the presence of non-birefringent spherulites as a result of the mixed growth. Although this phenomenon has been reported,

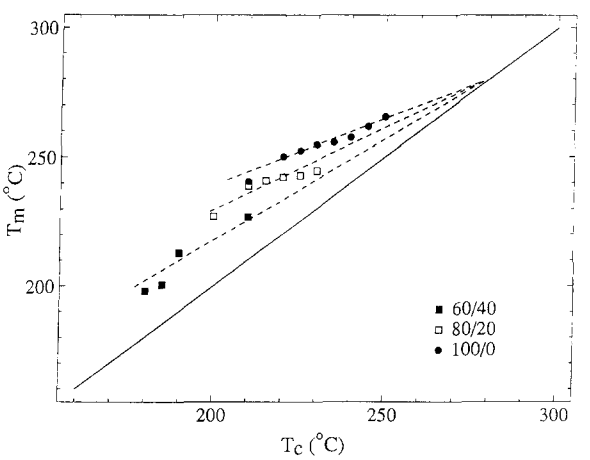

Figure 16 Hoffman–Weeks plot (T_m vs. T_c) of data retrieved from *Figure 15*. The $T_c + 10°C$ melting peak is excluded here

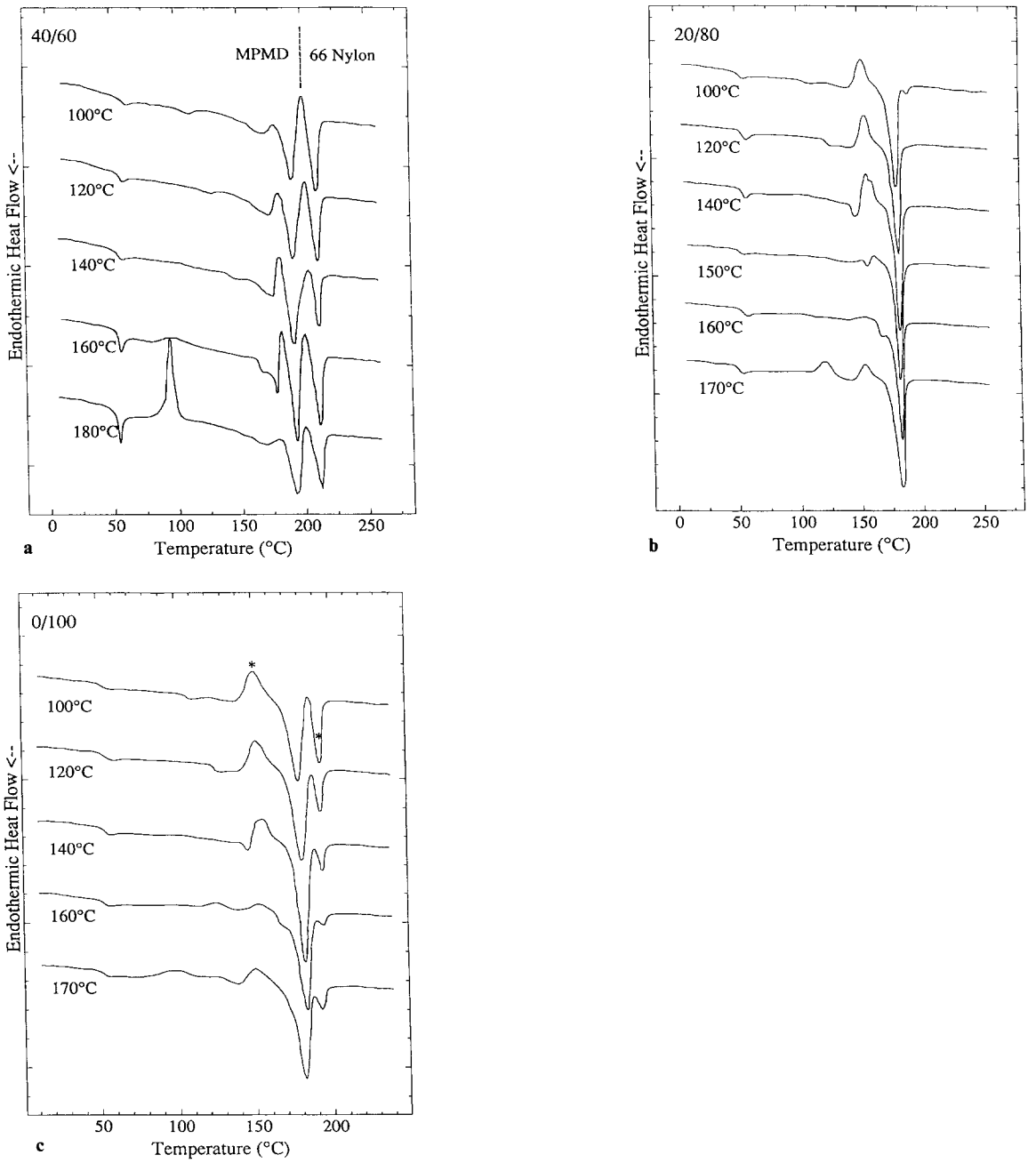

Figure 17 D.s.c. scans of isothermally crystallized samples at different temperatures for the compositions of (a) 40/60, (b) 20/80 and (c) 0/100

we could not identify such a morphology in any composition.

For all compositions, spherulite aggregates can be observed at higher crystallization temperatures. These aggregates may be mixed with the positive or negative spherulites in the high 66 compositions, or with the spiral spherulites in the low 66 compositions. A typical aggregate morphology for the 20/80 composition in *Figure 13*. These spherulites have complex optical properties and grow at twice the rate of their dominant counterparts. However, the optical melting point of the aggregates is similar to the latter. It has been shown, again, in nylon-6,6, that there is no preferred optical orientation of the unit cells in this morphology[17].

A schematic diagram of the sign of spherulite birefringence as a function of the temperature for different compositions is shown in *Figure 14*. It is clear that the spherulite morphology of the higher 66 compositions ($\geq 60\%$) is similar to that of the nylon-6,6, whereas the morphology of the lower 66 compositions ($\leq 40\%$) is probably dominated by the MPMD-6 homopolyamide. The later morphology also showed a remarkable resemblance to that of the nylon-5,6, which is the same as MPMD-6 except for the absence of the pendent methyl group.

Melting behaviour

D.s.c. heating scans of isothermally crystallized samples with the compositions of 100/0, 80/20 and 60/40 are shown in *Figures 15a–c* respectively. In the case of 100/0 (nylon-6,6), multiple endotherms are observed as a

function of crystallization temperature T_c. For example, three endotherms are present at lower crystallization temperatures (210–230°C), whereas a single endotherm is found at the high temperature (250°C). The three endotherms show a consistent pattern at different temperatures, i.e. the lowest endotherm always occurs at about 10°C above T_c, the middle endotherm also increases with T_c but at a slower rate, and the highest endotherm remains relatively constant. The lowest endotherm is a general feature of isothermal crystallization (almost all polymers show a $T_c + 10$°C small endotherm when annealed at T_c), which is probably due to the melting of thin crystals formed during the space-filling crystallization[23]. In this case, the middle endotherm can be assigned as the melting of the 'regular' lamellae and the highest endotherm may be associated with the melting of recrystallized (reorganized) crystals with better perfection. In *Figure 15a*, we indicate the increasing trend of the middle endotherm with the symbol (●), and conclude that this endotherm may be related to the single endotherm at high T_c. A similar behaviour is also observed in the composition of 80/20 but not so obvious in 60/40 (*Figures 15b* and *c*). The Hoffman–Weeks plot using the middle endotherm in compositions 100/0 to 60/40 is shown in *Figure 16*. The highest endotherm (assigned as the melting of reorganized crystals) clearly decreases with the increasing MPMD content. However, the extrapolation of the equilibrium melting temperature T_m° by the interception of the linear relationship between T_m and T_c (dotted line) and the $T_m = T_c$ line shows a single value at 280°C for the three compositions. This value is consistent with the reported T_m° value of nylon-6,6[24–26]. The constant T_m° for three different compositions indicates that the temperature-dependent crystals have totally excluded the MPMD unit. This conclusion has also been drawn using *Figure 4*.

Figures 17a–c show d.s.c. scans of samples crystallized isothermally at different temperatures for the compositions of 40/60, 20/80 and 0/100 respectively. For simplicity, we will start the discussion with the scans of 0/100 (MPMD-6 nylon). In *Figure 17c*, it is clear that the annealing only eliminates the lower exotherm of form I. The higher exotherm (from form II) remains during the heating, and shows a similar enthalpy change as that of the higher endotherm (both indicated by the symbol *). When the T_c increases, both higher-temperature endotherm and exotherm decrease, indicating that formation of form I crystals increases. The Hoffman–Weeks plot for 0/100, again excluding the lower melting point associated with the $T_c + 10$°C endotherm, is shown in *Figure 18*. Very little increase in T_m by T_c is seen here, which indicates that the lamellar thickening effect is small for both forms I and II of MPMD-6 nylon. The extrapolated value of T_m° is 186°C for form I, and 195°C for form II. A similar behaviour is found in *Figures 17b* and *18* for the composition of 20/80. In fact, the melting points of 20/80 are superimposed on the data of 0/100 in *Figure 18* (naturally, the same T_m° values for forms I and II can be extrapolated). This indicates that 20/80 is dominated by the crystallization and melting behaviour of pure MPMD-6 nylon. In the case of 40/60, a complicated melting behaviour is seen in *Figure 17a*. Using the melting scans of 66 and MPMD-6 nylons as a base, we

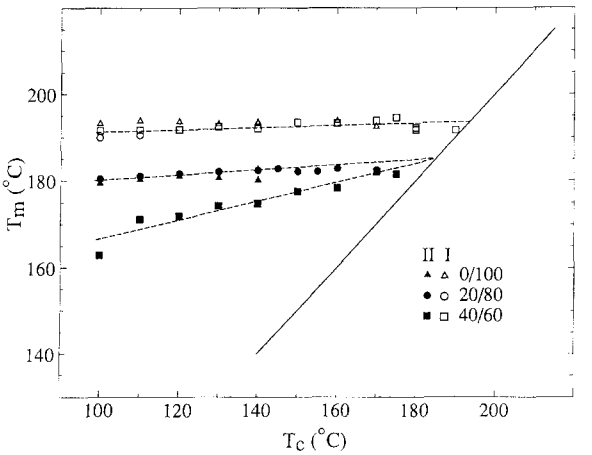

Figure 18 Hoffman–Weeks plot (T_m vs. T_c) of data retrieved from *Figure 17*. The $T_c + 10$°C melting peak is excluded here

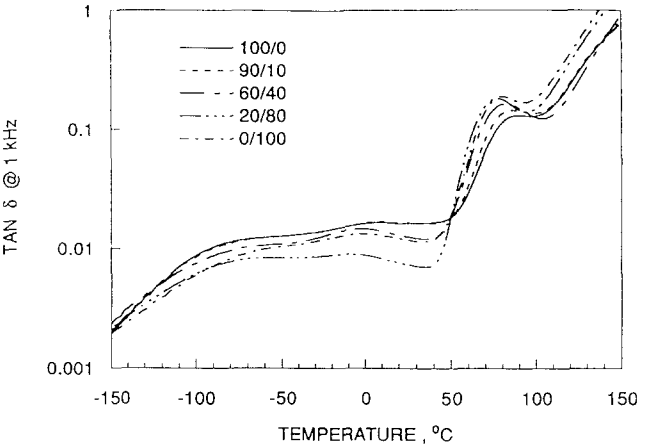

Figure 19 The dielectric dissipation factor at 1 kHz *versus* temperature for homopolymers of 66 and MPMD-6, and copolymers having 66/MPMD-6 ratios of 90/10, 60/40 and 20/80

have assigned the highest endotherm (above 200°C) to the melting of nylon-6,6 crystals, and the lower endotherms (below 200°C) to the melting of two MPMD-6 polymorphs. The highest endotherm in 40/60 is found to follow the decreasing trend of the highest endotherm by increasing MPMD content in 100/0 to 60/40 (*Figure 15*) as expected. On the other hand, the extrapolated T_m° values for both polymorphs in 40/60 is consistent with those in 20/80 and 0/100 (*Figure 18*).

In summary, from the d.s.c. scans of the isothermally crystallized samples for different compositions, we conclude that the compositions of 80/20 and 60/40 are dominated by the crystallization and melting behaviour of nylon-6,6; the 20/80 composition is dominated by MPMD-6 nylon; whereas 40/60 shows a mixture of 66 and MPMD-6 nylon crystals.

Properties of the amorphous phase

The viscoelastic relaxations in polyamides are generally considered to be properties of the amorphous portions[27]. These relaxations were studied by dielectric measurements at frequencies from 10 to 10^5 Hz. In *Figure 19*, the dissipation factor at 1 kHz is plotted on a logarithmic scale against temperature for homopolymers of 66 and MPMD-6 as well as copolymers having

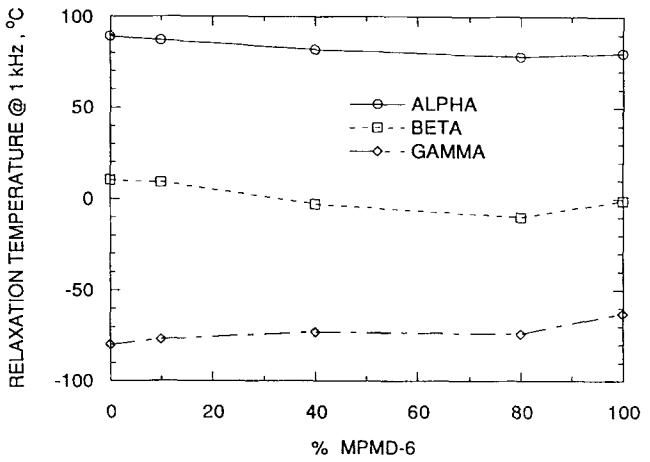

Figure 20 Relaxation temperature at 1 kHz *versus* composition for the dielectric relaxations

66/MPMD-6 ratios of 90/10, 60/40 and 20/80. These samples had all been previously heated to 160°C to remove moisture and increase crystallinity.

The incorporation of MPMD-6 increases the dissipation factor in the region of the alpha relaxation, which is observed near 90°C, and lowers it in the region of the lower-temperature secondary relaxations. The increase in the dissipation factor at temperatures above the alpha relaxation is attributed to ionic conductivity.

The alpha and beta relaxations appear as maxima in isochronal temperature scans. The gamma relaxation, which is seen only as a shoulder in these scans, does give maxima in isothermal frequency scans. As shown in *Figure 20* and *Table 3*, the incorporation of MPMD decreases the temperatures of the alpha and beta relaxations and increases the temperature of the gamma relaxation. Each of the relaxations appears at a higher temperature in the MPMD-6 homopolymer than in the 20/80 copolymer.

The apparent activation energy for the alpha relaxation decreases with increasing levels of MPMD from 96 kcal mol^{-1} for the 66 homopolymer for 64 kcal mol^{-1} for MPMD-6. The activation energies for the secondary relaxations do not vary significantly with composition, being about 15 kcal mol^{-1} for the beta relaxation and 11 kcal mol^{-1} for the gamma relaxation.

The greater loss of MPMD-6 in the region of the alpha relaxation may reflect a larger amorphous fraction. With respect to the lower-temperature relaxations, it should be noted that both polymers are based on adipic acid. Studies by n.m.r. and molecular modelling have shown that, in nylon-6,6 at low temperatures, the local motions in the acid moiety are more active than in the diamine moiety[28]. Therefore, it is not entirely surprising that the low-temperature internal motions should be dominated by the common structural feature. The fact that the low-temperature dielectric loss is slightly lower in polymers containing MPMD suggests that the motions in the diamine moiety are smaller in the case of MPMD than in HMD.

It is clear, however, that the properties of the amorphous portions of these isomeric polymers are much more similar than those of their crystals.

CONCLUSIONS

While both 66 and MPMD-6 can crystallize, they do not co-crystallize. This is probably due to their different repeat lengths and the fact that they are even–even and odd–even polyamides, respectively. MPMD-6 crystallizes much more slowly and can be quenched to an essentially amorphous state. It has two crystalline forms, which crystallize and melt separately. Both homopolymers as well as their copolymers exhibit a rich variety of spherulitic structures and very different crystallization and melting properties.

All of the polymers in this family have generally similar dielectric properties, indicating that the variations in molecular structure have a smaller effect on the amorphous regions than on the crystals. The incorporation of MPMD increases the dielectric loss in the region of the alpha relaxation, probably because of the larger amorphous content. However, the low-temperature dielectric relaxations are somewhat weakened.

ACKNOWLEDGEMENTS

The authors thank E. N. Blanchard, W. G. Kampert, J. P. McKeown and J. R. Dowell for their technical assistance. Dr D. N. Marks synthesized the polymers and Dr C. Jackson did the g.p.c. analysis. The room-temperature X-ray diffraction analysis was conducted by Dr K. H. Gardner and J. E. Freida. Portions of the thermal analysis work were contributed by Dr M. M. Keating and R. Kovelski.

Table 3 Temperatures (°C) at 1 kHz of dielectric relaxations

	Relaxation		
66/MPMD-6 ratio	Alpha	Beta	Gamma
100/0	89	10	−88
90/10	87	9	−77
60/40	82	−3	−73
20/80	78	−10	−74
0/100	80	−1	−63

REFERENCES

1 Jones, G. A. and Starkweather, H. W. *J. Macromol. Sci.–Phys. (B)* 1985, **24**, 131
2 Bunn, C. W. and Garner, E. V. *Proc. R. Soc. (A)* 1947, **189**, 39
3 Flory, P. J. *J. Chem. Phys.* 1947, **15**, 684; 1949, **17**, 223
4 Flory, P. J. 'Principles of Polymer Chemistry', Cornell University Press, Ithaca, NY, 1953, p. 570
5 Starkweather, H. W., Zoller, P. and Jones, G. A. *J. Polym. Sci., Polym. Phys. Edn.* 1984, **22**, 1615
6 Walter, E. R. and Reading, F. P. *J. Polym. Sci.* 1956, **21**, 561
7 Cole, E. A. and Holmes, D. R. *J. Polym. Sci.* 1960, **46**, 245
8 Sivan, P. R. *J. Polym. Sci.* 1962, **56**, 409
9 Baker, C. H. and Mandelkern, L. *Polymer* 1966, **7**, 71
10 Richardson, M. J., Flory, P. J. and Jackson, J. B. *Polymer* 1966, **7**, 221
11 Predy, J. E. and Wheeler, E. J. *Makromol. Chem.* 1977, **178**, 2461
12 Starkweather, H. W. and Jones, G. A. *J. Polym. Sci., Polym. Phys. Edn.* 1981, **19**, 467
13 Starkweather, H. W. and Moynihan, R. E. *J. Polym. Sci.* 1956, **22**, 363
14 Lindegren, C. R. *J. Polym. Sci.* 1961, **50**, 181
15 Khoury, F. *J. Polym Sci.* 1958, **27**, 389
16 MaGill, J. H. *J. Polym. Sci. (A)* 1965, **3**, 1195
17 MaGill, J. H. *J. Polym. Sci. (A-2)* 1966, **4**, 243

18 MaGill, J. H. *J. Polym. Sci. (A-2)* 1969, **7**, 123
19 Hoffman, J. D. *SPE Trans.* 1964, 315
20 Clark, E. S. and Wilson, F. C. 'Nylon Plastics' (Ed. M. I. Kohan), Wiley, New York, 1973, Ch. 8
21 Mann, J. and Roldan-Golzalez, L. *J. Polym. Sci.* 1962, **60**, 1
22 Koenig, J. L. and Agboatwalla, M. C. *J. Macromol. Sci. (B)* 1968, **2**, 391
23 Hsiao, B. S., Gardner, K. H., Wu, D. Q. and Chu, B. *Polymer* 1993, **34**, 3986
24 Wunderlich, B. 'Macromolecular Physics', Academic Press, New York, 1980, Vol. 3, p.57
25 Illers, K. H. and Haberkorn, H. *Makromol. Chem.* 1971, **146**, 267
26 Illers, K. H. *Prog. Colloid Polym. Sci.* 1975, **58**, 61
27 McCrum, N. G., Read, B. E. and Williams, G. 'Anelastic and Dielectric Effects in Polymeric Solids', Wiley, New York, 1967
28 Wendoloski, J. J., Gardner, K. H., Hirschinger, J., Minra, H. and English, A. D. *Science* 1990, **247**, 437